

COMPARISON OF 1D VS 2D VS 3D NUMERICAL APPROACHES FOR PREDICTION OF SEISMIC GROUND MOTION AND SITE EFFECTS IN THESSALONIKI URBAN AREA

Kiana HASHEMI¹, Chiara SMERZINI²

ABSTRACT

This study aims at comparing 1D, 2D and 3D numerical approaches to predict site effects in the metropolitan area of Thessaloniki, Northern Greece. The availability of detailed geotechnical/geophysical data together with the seismological information regarding the relevant fault sources allowed the construction of a large-scale 3D numerical model suitable for generating physics-based ground shaking scenarios within the city of Thessaloniki. The results of such study then are used for performing site response analysis in the Thessaloniki urban area based on the numerical simulations of earthquake ground motion during the Volvi 1978. The results in terms of ground motion amplification functions obtained with 1D, 2D and 3D numerical approaches have been compared with the ones obtained from earthquake recordings.

Keywords: site effects; numerical simulation; plane wave propagation; Domain Reduction Method

1. INTRODUCTION

Site effect and local soil conditions have been known to have crucial impact on the estimation of earthquake ground motion and seismic hazard assessment. Standard approaches based on 1D or rarely-used 2D description of seismic wave propagation cannot predict the complexity in seismic amplification patterns arising from the seismic source and near-surface geology (Smerzini et al. 2011; Olsen et al. 2000). However, 3D numerical simulation has demonstrated to have great potentialities for estimation of seismic ground motion and of its spatial variability, especially in near-fault conditions, for extreme events and complex site properties. Therefore, this paper aims at comparing 1D, 2D, and 3D approaches at predicting site effects in the metropolitan area of Thessaloniki, Northern Greece. For broader area of Thessaloniki, a full 3D numerical simulation of seismic wave propagation has been recently conducted by Smerzini et al. (2016). The results of this study will be used for performing site response analysis in the Thessaloniki urban area based on different numerical approaches. Namely, the results of numerical simulations of earthquake ground motion during the Volvi 1978 earthquake from the following numerical models will be compared: i) 3D soil model in Thessaloniki metropolitan area with a 3D kinematic characterization of the seismic source; ii) 2D models of a representative cross-section of the basin under vertical plane-wave propagation, using, as input, the output of the 3D simulation at outcropping bedrock; iii) 1D model under vertical plane-wave propagation, using the same input as for point (i). The 2D and 3D numerical simulations presented in this paper have been carried out by an open-source software package SPEED (*S*pectral *E*lement in *E*lastodynamics with *D*iscontinuous *G*alerkin) based on a discontinuous Galerkin spectral element method. The simulation of the 2D plane wave propagation in SPEED is performed through the implementation of a well-known *sub-structuring* technique called Domain Reduction Method, DRM (Bielak et al., 2003).

¹Ph.D., Studio Geotecnico Italiano Srl., Milan, Italy, k.hashemy@studiogeotecnico.it

²Researcher, Politecnico di Milano, Milan, Italy, chiara.smerzini@polimi.it

2. SEISMOTECTONIC AND GEOLOGIC CONTEXT OF THESSALONIKI BROADER AREA

The city of Thessaloniki is the second largest city in Greece and a major international port that constitutes the center of merchant shipping for the Balkan countries. Thessaloniki is located on the Axios-Vardar zone, adjacent to the Servomacedonian continental margin, which is one of the most seismotectonically active zones in Europe. A large portion of the seismicity of this area is associated to the Mygdonia graben which is around 25 km northeast of Thessaloniki and where a destructive earthquake on 20 June 1978 with moment magnitude M_w 6.5 occurred. The 1978 earthquake caused extensive damage to many villages located close to the epicentral area (Stivos, Scholari, Peristeronas, Gerakarou), as well as in Thessaloniki, where the death toll reached the value of 45 people. This earthquake has been considered as the first earthquake with a serious impact on a big modern urban center in Greece. Based on the historical data, the study area is characterized by moderate to large seismic activity associated mainly to the Mygdonia Basin and the Anthemountas fault zone, with magnitude up to $M_w=6.5$.

From a geological point of view, the Thessaloniki urban area is characterized by three main geological structures: rocks (gneiss, epigneiss and green shists); sedimentary deposits dominated by the stiff red silty clays, covering the bedrock basement beneath the city; recent generally soft deposits consisting of clays, sands and pebbles. The definition of 3D thematic maps of these geological formations together with their geotechnical/geophysical characterization was addressed, first, by Anastasiadis et al. (2001) and, subsequently, by Apostolidis et al. (2004). The latter had estimated 1D shear wave (V_s) profiles up to a depth of about 300 m at 16 sites in the broader area of Thessaloniki, applying the spatial autocorrelation coefficient method (SPAC) method to array measurements of microtremors. Combining these new data with the geotechnical maps from Anastasiadis et al. (2001), the authors identified five soil formations and proposed updated 3D thematic maps of the geotechnical/geophysical model applicable to the urban area of Thessaloniki.

3. NUMERICAL APPROACH FOR 3D AND 2D (DRM) WAVE PROPAGATION

The 2D and 3D numerical simulations presented in this paper have been carried out by the open-source software package SPEED (*S*pectral *E*lement in *E*lastodynamics with *D*iscontinuous *G*alerkin), using the Discontinuous Galerkin Spectral Elements Method (DGSEM). SPEED can handle the simulation of large-scale seismic wave propagation problems including the coupled effect of a seismic fault rupture, the propagation path through Earth's layers and localized geological irregularities, such as alluvial valleys. Based on a discontinuous version of the classical spectral element (SE) method, as explained in Antonietti et al. (2012), SPEED is naturally oriented to solve multi-scale numerical problems, allowing one to use non-conforming meshes (h -adaptivity) and different polynomial approximation degrees (N -adaptivity) in the numerical model. The code has been optimized to run on multi-core computers and large clusters (e.g., Fermi BlueGene/Q at CINECA), taking advantage of the hybrid MPI-OpenMP parallel programming. The reader is referred to Mazzieri et al. (2013) and to the SPEED website, <http://speed.mox.polimi.it/>, for an extensive explanation of the mathematical framework of the method, the code features and its main applications.

In order to compare the performance of different numerical approaches for predicting the main features of the seismic ground motion and site effects in Thessaloniki urban area, reference has been made to the M_w 6.5 June 20 1978 Volvi earthquake which was one of the earthquakes with greatest impact on the city of Thessaloniki.

3.1 3D Spectral element model

Based on the available data regarding both the characterization of the seismic sources and geological, geotechnical and geophysical aspects, a large-scale 3D numerical model was constructed by using SPEED and discussed in detail in Smerzini et al. (2016). The 3D numerical model has been constructed including the following features: i) ground topography; ii) kinematic finite-fault rupture

model for the 1978 earthquake with a self-similar slip model (k^{-2} model) according to Herrero and Bernard (1994); iii) a horizontally-layered crustal model for deep rock materials (from Ameri et al., 2008); iv) 3D soil model of the Thessaloniki bay area, based on the works by Anastasiadis et al. (2001) and Apostolidis et al. (2004); v) an hexahedral unstructured numerical mesh including both the Thessaloniki bay area and the fault; (vi) a linear visco-elastic material behavior with a Q factor proportional to frequency.

The constructed 3D mesh is illustrated in Figure 1. The mesh extends over a volume of about $82 \times 64 \times 31 \text{ km}^3$ and is discretized using an unstructured hexahedral conforming mesh with characteristic element size ranging from a minimum of $\sim 150 \text{ m}$ at ground surface inside the basin to 2000 m at the bottom of the model. Note that the mesh incorporates also the geometry of four seismogenic fault sources posing hazard to the city of Thessaloniki, specifically, Gerakarou (i.e., the fault responsible of the 1978 Volvi earthquake), Langadhas, Angelochori and Souroti (the latter two being part of the Anthemountas fault system). The model consists of 753,211 spectral elements, resulting in approximately 60 million of total degrees of freedom, with a third order polynomial approximation degree. Considering a rule of thumb of 5 grid points per minimum wavelength for non-dispersive wave propagation in heterogeneous media by the SE approach, this model can propagate frequencies up to about 1.5 Hz .

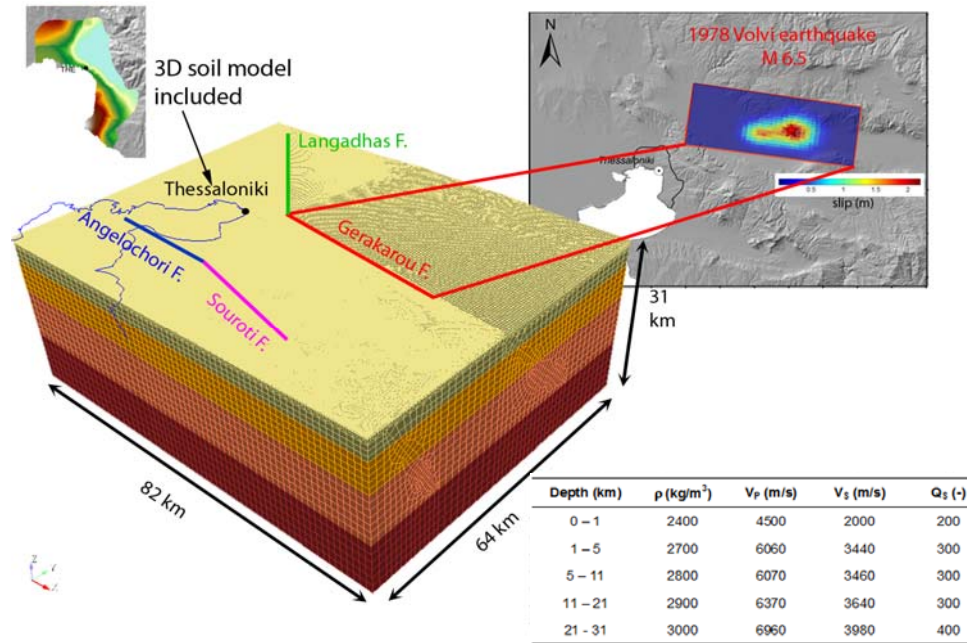


Figure 1. 3D spectral element mesh for the broader Thessaloniki area (adapted from Smerzini et al., 2016). The crustal model and the faults included in the model area also shown.

As regards the 3D soil model, two generic homogeneous soil profiles with linear visco-elastic behavior were defined for the alluvial deposits overlying the bedrock for sites belonging to Eurocode 8 - EC8 (CEN, 2004) ground category B (average shear wave velocity in the top 30 m , $V_{S30} = 360\text{--}800 \text{ m/s}$) and C ($V_{S30} = 180\text{--}360 \text{ m/s}$), after Pitilakis et al. (2015).

The soil profiles in terms of S- and P- wave velocity (V_S and V_P , respectively), soil density (ρ) and quality factor (Q_S), are given in Figure 2. The functional form for the V_S/V_P gradient, $V_{(S/P)}(z) = V_{(S/P,l)} + (V_{(S/P,m)} - V_{(S/P,l)})(z/h)^{0.70}$, with $V_{S,l} = 500 \text{ m/s}$ being the lower V_S at ground surface for soil category B (or 300 m/s for soil category C) and $V_{S,m} = 2000 \text{ m/s}$ the upper V_S at top of geologic bedrock and $V_{P,l} = 2000 \text{ m/s}$ (or 1800 m/s for soil category C) and $V_{P,m} = 4500 \text{ m/s}$ being the minimum and maximum P wave velocity, respectively, with $h =$

1000 m, was defined according to the recent findings achieved in the framework of NERA project, based on empirical data from SHARE-AUTH database (Pitilakis et al., 2014).

Note that these generic soil profiles are consistent with the site response information made available from numerous fundamental frequency (H/V) measurements performed within Thessaloniki (e.g. Triantafyllidis et al. 1999). A linear visco-elastic material with a frequency proportional quality factor for a reference frequency of 0.67 Hz has been assumed. As discussed in details in Smerzini et al. (2016), the choice of Q_S profile has been made on one side, by considering the average values provided by Anastasiadis et al. (2001) for the main sediment formations present in the city and, on the other side, by constraining its behavior with depth on the basis of the relationships typically adopted in the literature, according to which Q_S can be reasonably estimated as $V_S/10$ (see e.g. Maufroy et al., 2015; Paolucci et al., 2015). Although the analysis of the impact of a frequency proportional Q factor, with respect to a frequency constant Q , has been not specifically addressed in this work, such an assumption is expected to have a minor influence on results because of the limited range of frequencies (up to 1.5 Hz) and distances (up to about 30 km) under consideration.

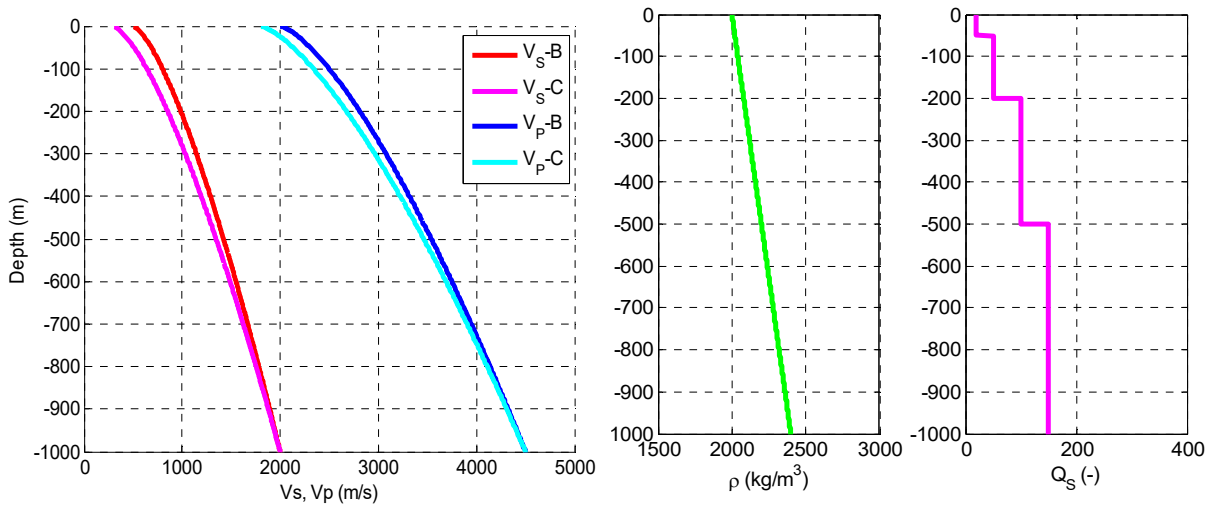


Figure 2. Calibration of average soil profiles in terms of V_S , V_P , ρ and Q_S (at a reference frequency $f_0 = 0.67$ Hz) for the 3D model, based on the available 1D data.

3.2 Kinematic modeling of the seismic source

For the simulation of the Volvi 1978 earthquake, the kinematic source model rupturing the Gerakarou fault has been considered with a k^{-2} slip model with location and size of the asperities resembling the main slip patch of the model published by Roumelioti et al. (2007). The final kinematic source parameters are listed in Table 1 while the slip distribution as well as the 3D numerical model is plotted in Figure 1.

Table 1. Kinematic source parameters for the simulation of the 1978 Volvi earthquake. Geographic coordinates are in WGS84.

Hypocenter	Depth	$L \times W$	Z_{top}	Strike	Dip	Rake	Rupture	Rise
(°N, °E)	(km)	(km ²)	(km)	(°)	(°)	(°)	Vel (km/s)	Time (s)
(40.705, 23.266)	7.5	35 × 19	1	278	46	-70	2.6	0.6

3.3 2D modeling of the seismic response across a representative cross-section

For the 2D modeling of the seismic response in Thessaloniki metropolitan area, a 2D representative cross-section of the Thessaloniki urban area is selected and studied in detail, based on the same constructed 3D numerical model. The location of the selected cross-section (section AA') in the geological map of the Thessaloniki metropolitan area as well as in the 3D numerical model is presented in Figure 3. Note that the cross-section AA' passes through two accelerometric stations ROT and LEP. The spectral element mesh for such a cross-section is illustrated in Figure 4.

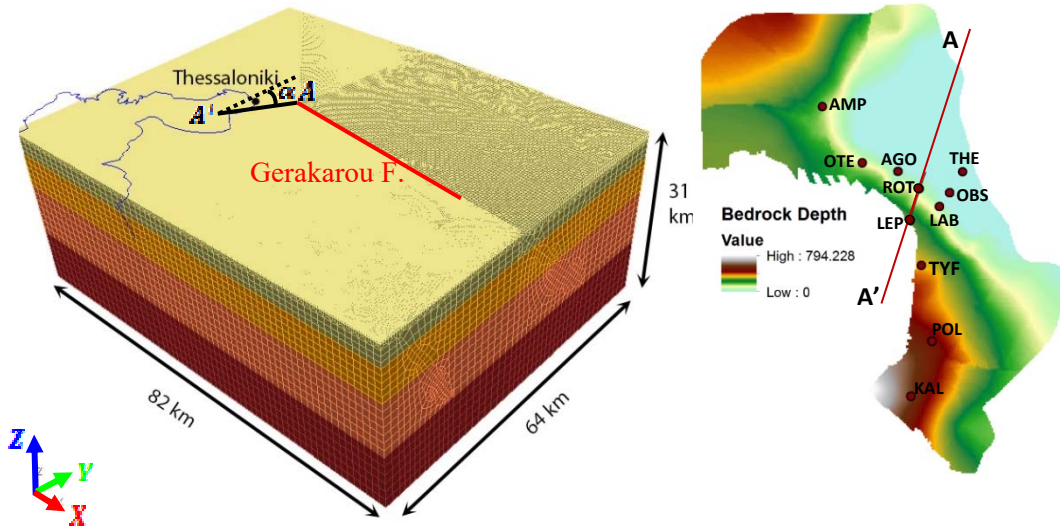


Figure 3. *Left*: 3D numerical model of the Thessaloniki broader area used for deriving the 2D reduced model of the cross-section AA'. α denotes the angle of rotation of the cross-section with respect to y axis. *Right*: The map showing the depth of geologic bedrock (Apostolidis et al., 2004) within the city of Thessaloniki.

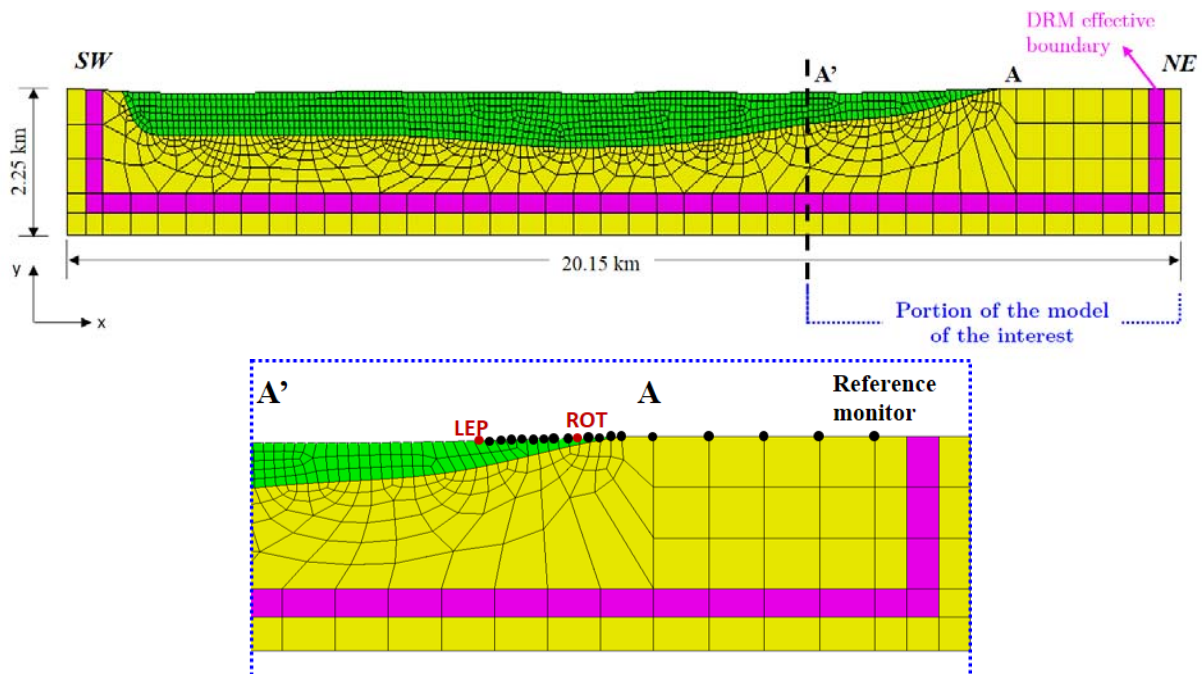


Figure 4. Top: 2D reduced model corresponding to cross-section AA' passing through the Thessaloniki metropolitan area. The green area shows the alluvial basin while the yellow corresponds to the bedrock (see Table 2). Bottom: The localized area of the interest with the positions of the output receivers selected for 2D site-specific analysis. The filled red dots show the location of the accelerometric stations ROT and LEP while "Reference monitor" refers to the input motion on the outcropping bedrock (derived from the 3D simulations). The DRM effective boundary refers to a strip of elements where the free-field solution is applied and is defined

on both sides of the basin.

It is worth underlining that the basin, which is open to the SW, has been artificially closed to allow the application of the DRM. As a matter of fact, a strip of elements where the free-field solution is applied (called DRM effective boundary in Figure 4) needs to be defined on both sides of the basin. However, the model has been extended about 16.5 km with respect to the original length of the cross-section to be sure to limit any effect of the spurious reflections on the localized area of interest. The yellow and green areas in Figure 4 refer to the alluvial basin and rock, respectively, the properties of which are defined in Table 2. Note that the selected dynamic properties are identical to the ones assumed in the 3D numerical model for comparison purposes. The localized area of interest is zoomed in Figure 4 to illustrate the positions of the output receivers for 2D site-specific analysis: the filled red dots denote the location of the strong ground motion stations ROT and LEP, while the *Reference monitor* refers to a node on the outcropping bedrock where the input motion with time dependence provided by the 3D numerical simulation has been applied.

Table 2. Dynamic properties of the reduced model of the 2D cross-section of the Thessaloniki urban area where NH referred to the variation of properties of soil being assigned with respect to depth (see Figure 2).

Layer	$V_F \left(\frac{m}{s}\right)$	$V_S \left(\frac{m}{s}\right)$	$\rho \left(\frac{kg}{m^3}\right)$	$f_{max} (Hz)$	Q
Basin	NH	NH	NH	2	NH
Halfspace	4500	2000	2400	2	200

The simulation of the plane wave propagation in SPEED is performed through the implementation of a *sub-structuring* technique called the Domain Reduction Method, DRM (Bielak et al., 2003, Faccioli et al., 2005, Scandella, 2007). This approach subdivides the problem into two sequential models with different scale dimensions. In the first model, the geological feature of interest will be removed and the free-field ground motion (the ground motion in absence of the localized structure) in halfspace due to the defined seismic source will be computed. In the second step, the reduced numerical model which encompasses the geological feature of interest (e.g., structure, basin or topographic irregularity) is generated excluding the seismic source and most of the propagation path from source to site. In this phase, the seismic excitation is introduced as a set of effective nodal forces evaluated based on the free-field ground displacements calculated at the first step and will be applied within the fictitious strip of elements that separates the exterior domain from the interior one.

In SPEED, the effective nodal forces are computed through the analytical free-field solution for P-SV-SH plane wave propagation with arbitrary angle of incidence γ through horizontally layered soil media. These analytical solutions are computed through the Haskell-Thomson (H-T) propagation matrix method (Haskell, 1953, Thomson, 1950). For a generic input motion where both P and S wave components are simultaneously present, there is a need for performing two independent numerical analyses and a suitable superposition approach to combine the results. For this objective, a convolution process based on the concept of 2D transfer function matrix proposed by Paolucci (1999) is suggested which will be relevant only for linear elastic behavior where the superposition principle applies. If we denote the SV and P in-plane components of motion by u_{SV} and u_P respectively, the frequency response at a given receiver k on the ground surface due to an input harmonic motion of the W type ($W = SV, P$) along the i^{th} direction (for $i=1, 2, \dots$, Cartesian axis) can be expressed by means of the transfer function matrix H^k_{iW} , as follows:

$$\begin{bmatrix} Y_1(f) \\ Y_2(f) \end{bmatrix}^{(k)} = \begin{bmatrix} H_{1SV}(f) & H_{1P}(f) \\ H_{2SV}(f) & H_{2P}(f) \end{bmatrix}^k \begin{bmatrix} U_{SV}(f) \\ U_P(f) \end{bmatrix} \quad (1)$$

where $Y_i(f)$ represents the frequency response in i^{th} direction, either in-plane horizontal ($i=1$) or in-

plane vertical ($i=2$), and U_W is the reference input ground motion of the W type at the reference site. After computing the transfer function matrix H for a generic site k , the 2D response of the model can be easily evaluated for any input motion under the assumption of linear elastic behavior.

Following this approach, two independent numerical analyses by SPEED have been performed for plane wave propagation polarized in P and SV directions with a Ricker wavelet input motion with maximum frequency $f_{max} = 2 \text{ Hz}$. Based on the results of these two simulations, the transfer function matrix of Eq. (1) has been indeed computed for each receiver of interest. After that, the output ground response can be achieved by performing the convolution procedure defined in Eq. (1), where the input motion U_W will be the displacement time histories from the 3D numerical analysis at outcropping bedrock. Specifically, the 3D time histories obtained at *Reference monitor* with location shown in Figure 4 have been considered after a proper rotation of the horizontal components in the plane of the cross-section. Finally, the response in time domain will be achieved by inverse Fast Fourier Transform (iFFT). It should be remarked that the 2D seismic response has been considered under the hypothesis of vertical plane wave incidence.

4. COMPARISON OF 1D VS. 2D VS. 3D NUMERICAL RESULTS

Figure 5 shows the comparison between 2D numerical analysis under the vertical plane wave incidence (black line) and the 3D numerical simulation (red line) in terms of displacement time histories in horizontal u_x and vertical u_y directions. These time histories are plotted for series of receivers equally spaced along the cross-section AA' . It is clear that the arrival of the waves at the basin stations is delayed in 3D case with respect to the 2D analysis. For instance, at the recording station LEP, there is a considerable difference between the two approaches in terms of times of wave arrivals. This effect can be related to the fact that in the 2D vertical wave propagation analysis, at the initial time of $t = 0$, the input motion is already right below the station while in the 3D simulation the propagation path is longer. In addition, it seems that the 2D plane wave propagation tends to slightly underestimate the level of ground motion with respect to the 3D simulation results especially when the depth of the soft sediments increases.

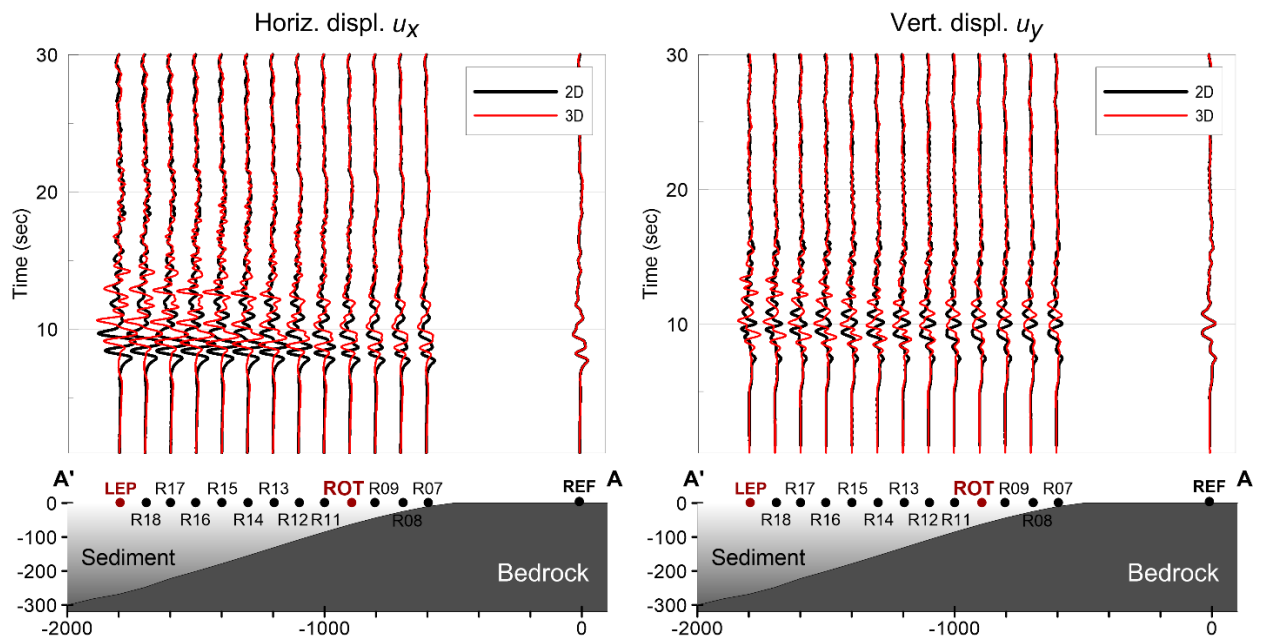


Figure 5. Comparison of displacement time histories obtained by the 2D numerical analysis under vertical plane wave incidence (black line) and the 3D physics-based simulation (red line). The results are presented for horizontal in-plane (parallel to section) as well as vertical in-plane (upward) components for series of receivers

aligned along AA' cross-section. The positions of those receivers are plotted in the bottom panel.

To highlight the amplification of ground motion due to the basin effect alone, Standard Spectral Ratios (referred to hereafter as *SSRs*), which is the Fourier spectral ratio of a selected receiver with respect to the reference station on outcropping bedrock, have been computed for the Geometrical mean of horizontal components (GMH), see Figure 6. The *SSRs* obtained by the 2D numerical analyses under the vertical plane wave incidence (gray line) are compared with the ones computed by the 3D numerical model (black line) for the same sites. It is found that, although 2D simulations predict amplification functions which are in agreement with 3D results over a broad range of frequencies (0-1 Hz), 2D plane wave incidence may underestimate the levels of spectral amplification at frequencies around 1-2 Hz and specifically for stations LEP and R17 while for other stations where the depth of the basin is not significant, 2D and 3D methods are in agreement in the frequency range of the numerical simulation.

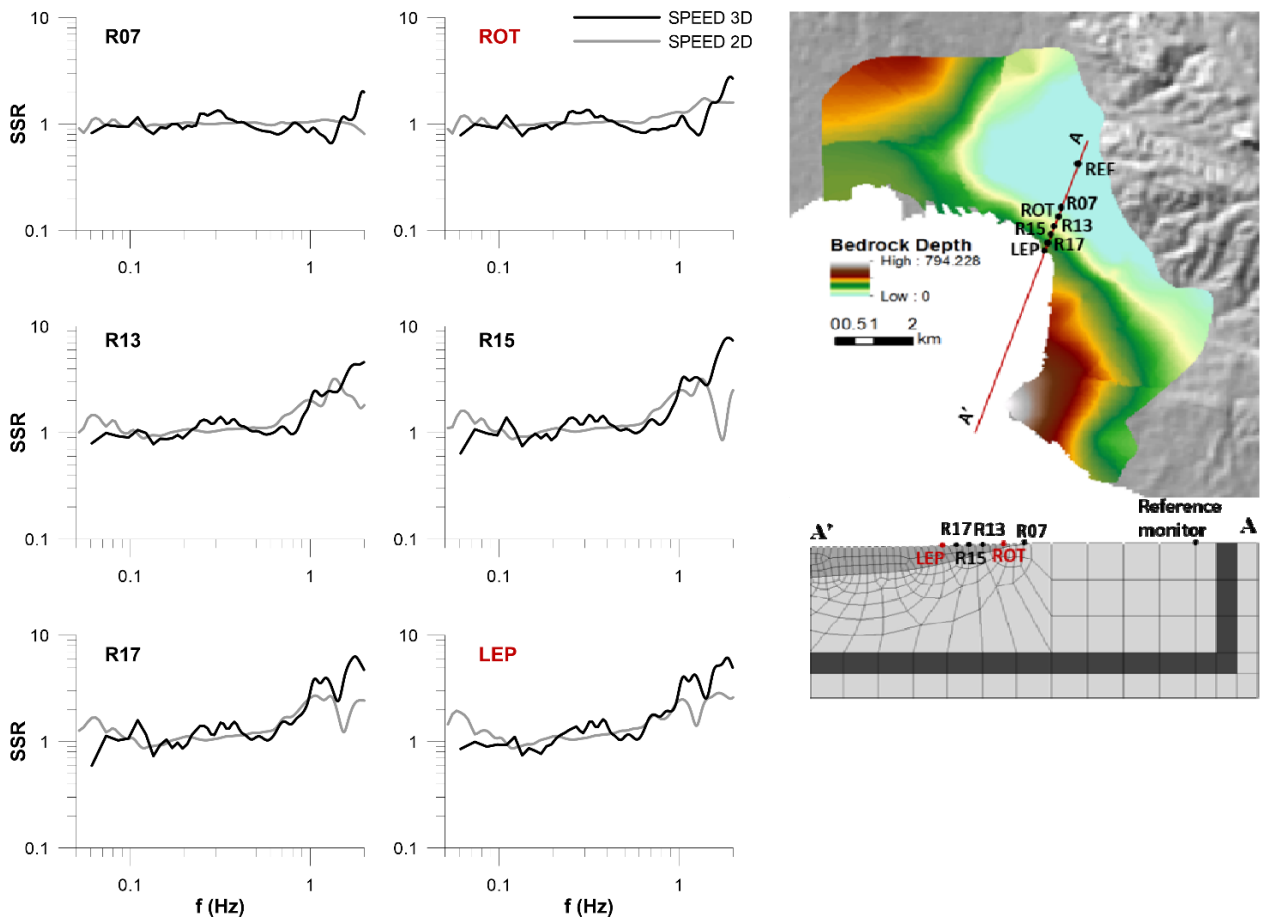


Figure 6. *Left*: *SSRs* (Standard Spectral Ratio) in a set of receivers located along the AA' cross-section with respect to the reference monitor on the outcropping bedrock for the Geometrical mean of horizontal components (GMH); Comparison between 3D (black line) and 2D numerical simulation under vertical wave incidence (gray line). *Right*: The location of receivers on the geological map of the Thessaloniki metropolitan area (*top* panel) as well as on the 2D numerical model (*bottom* panel).

Finally, a systematic comparison of 3D, 2D numerical and 1D approaches to predict site effects is shown for two representative stations, namely, ROT and LEP, in terms of amplification functions (*SSRs*) and displacement time histories (see Figure 7 and Figure 8, respectively). As previously done, the amplification function is computed as ratio of the Fourier spectrum at these two stations over that of a nearby rock reference station.

The amplification functions achieved from these simulations have been compared with observed data

as well (see Figure 7). The observed amplification function has been obtained using earthquake recordings available from a temporary accelerometric network within the city (Lachet et al. 1996). The comparison between experimental and 3D amplification functions has been performed for a series of stations (eleven three-component seismological stations) in Smerzini et al. (2016), where the capability of the 3D numerical model to predict site response effects within the Thessaloniki urban area has been verified. Among those stations, the observed amplification functions at stations ROT and LEP have been compared in this study with the results of 3D, 2D and 1D analyses. In order to evaluate such site response at the available stations, the Standard Spectral Ratio (SSR) technique has been applied (Borcherdt, 1970) and, to this end, the station OBS, located on outcrop basement, is considered as reference motion. 3D synthetics have been obtained by rotation of the horizontal components along the considered cross-section and the corresponding SSRs have been calculated considering OBS station as the reference site. 2D simulated time histories instead, have been achieved by vertical plane wave incidence, using as input the output of the 3D simulations at REF station (see superimposed map on the right hand side of Figure 7 for the location of the reference site). Finally, the 1D amplification function refers to the 1D transfer function obtained by analytical solution for a horizontally-layered soil column beneath these two stations and the corresponding time histories computed by a suitable convolution process. Results have been band-pass filtered between frequencies of 0.05 and 2 Hz in which the latter is the maximum resolution of the numerical simulations (the range is illustrated with superposition of the dashed lines in Figure 7).

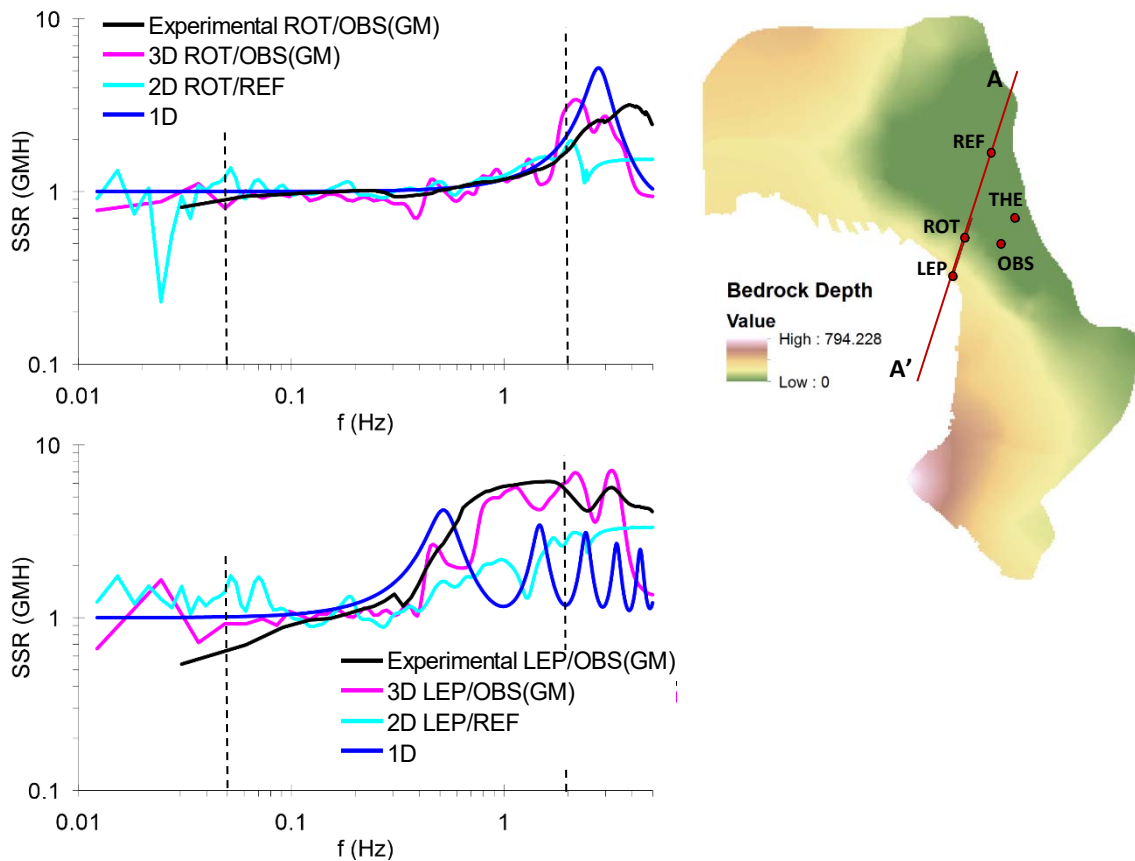


Figure 7. Comparison between experimental data and 3D, 2D and 1D simulation results in terms of SSR at ROT and LEP stations. Experimental and 3D results have been obtained with reference to OBS station while the 2D simulation refers to the results obtained by vertical plane wave incidence using, as an input, the output of 3D simulations at REF site. The 1D results refer to the 1D transfer function of a 1D soil column beneath these two stations. The map on the right hand side points out the location of the reference ground motions used to compute SSRs.

It is noted that for station ROT where the depth of basin is not significant, the SSR computed by 1D, 2D and 3D approaches in the frequency range of the numerical simulation are very close to the

observations. In any case, the amplitude is limited in the frequency range under consideration. However, for station LEP, where the amplification of the ground motion due to the presence of the basin is more pronounced and the amplitude of the *SSR* is larger, the discrepancies between the different modeling assumptions are larger. Specifically, the 3D simulation provides results close to the observations in terms of amplitude and spectral content. The numerical results as well as the observed data demonstrate amplification over a broad range of frequencies between 0.5 and 2.0 Hz, in which a major amplification of ground motion occurs at frequency of around 1.7 Hz with order of 6. Instead, both 2D and 1D simulations tend to underestimate the amplitude of the ground motion significantly, especially for frequencies larger than about 0.5 Hz. It is worth underlining that improved results for 2D simulations could be obtained by considering an oblique incidence from the North-East, which might lead to larger amplifications in between ROT and LEP stations.

It can be observed from Figure 8 that the ground motion time histories obtained by 2D and particularly 1D analysis illustrate significant amount of delay time with respect to the 3D simulation results as it has been mentioned before. Such delay can be referred to the differences in the simulation of incoming wavefield (extended source with obliquely incident waves in the 3D simulation vs the vertical incident wave in 2D and 1D analyses). It is also interesting to note that the level of complexity of seismic response introduced by 3D numerical modeling is much higher than that provided by 1D and 2D modeling. In fact, the contribution of higher vibration modes tends to spread the ground motion amplification over a much broader frequency range than in 1D and 2D.

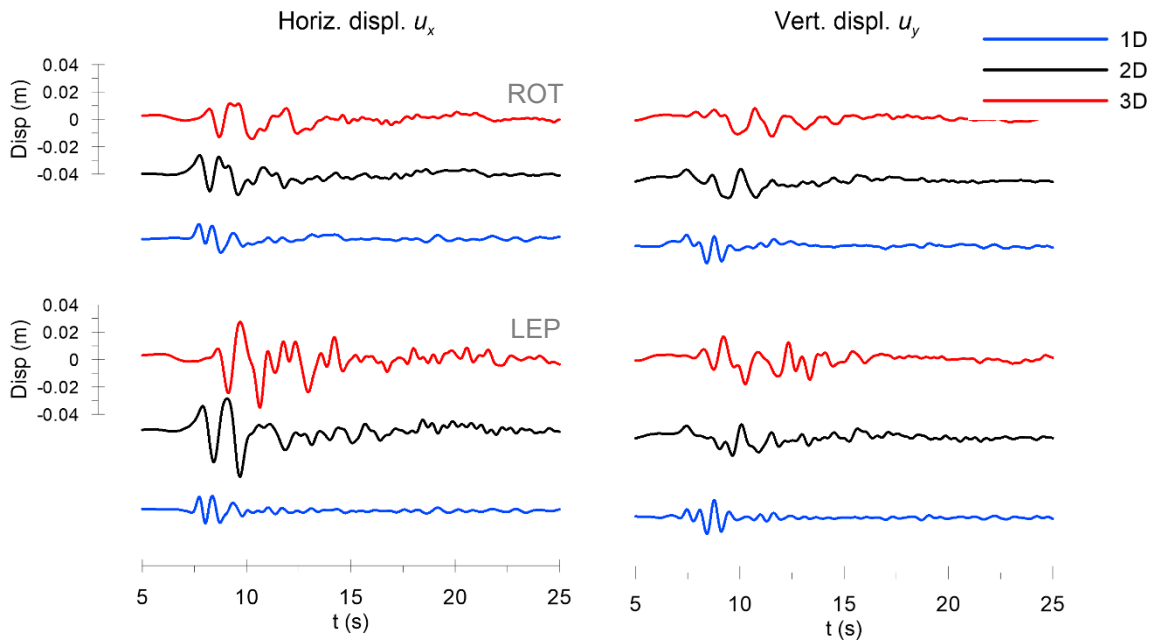


Figure 8. Comparison between 1D (blue line) analysis and 2D (black line) and 3D (red line) simulations at two representative stations, ROT (top panel) and LEP (bottom panel) located along the AA' cross-section, in terms of horizontal (left panel) and vertical (right panel) displacement time histories.

5. CONCLUSIONS

In this study, the performance of different numerical approaches to predict the variability of site amplification functions has been investigated, with application to the Thessaloniki urban area in Northern Greece. A critical comparison of the results of 3D numerical simulations of earthquake ground motion, including the full path of seismic waves from the source to the near-surface geology, with those obtained by simpler, standard, approaches, based on 2D and 1D seismic wave propagation, has been provided.

It has been shown that, despite the agreement between the basin-induced amplification function computed by 3D and 2D approaches in the low frequency range, the latter one underestimates the level

of the spectral amplification for $f > 0.5\text{-}1\text{ Hz}$, at least under the hypothesis of vertical wave incidence. The case of two representative sites within the city (LEP and ROT), for which a set of earthquake recordings is available, is discussed in more detail. For these sites, 3D amplification functions, computed for the M6.5 1978 Volvi scenario, turn out to be in reasonable agreement with the experimental ones, derived from the average of several observations with different magnitude and back-azimuths. Although such an agreement may be somehow related to the specificity of the considered 3D scenario, 2D and especially 1D approaches for ground response analyses are worse in predicting the observed frequency-dependent amplification features. It is noted, however, that improved 2D results may be obtained considering an oblique plane wave propagation from NE and this will be addressed in future work. Results of this study points out that coupling of seismic fault rupture effects with the complex local geology in a coupled 3D physics-based approach may be the key to explain the observed amplification features.

6. ACKNOWLEDGMENTS

This study has been carried out partially in the framework of the STREST Project “Harmonised approach to stress tests for critical infrastructures against natural hazards”, EU FP7/2007-2013, grant agreement no. 603389. The authors are indebted to the staff of the Aristotle University of Thessaloniki (AUTH) Scientific Computing Center (SCC) for allowing the extensive use of the AUTH cluster and for providing technical support. We also deeply thank Roberto Paolucci from Politecnico di Milano and Kyriazis Pitilakis from AUTH for the thoughtful remarks and criticism that helped improving this work. The cooperation of Ilario Mazzieri for technical support for conducting numerical simulation using SPEED is also gratefully acknowledged.

7. REFERENCES

- Ameri G, Pacor F, Cultrera G, Franceschina G (2008). Deterministic Ground-Motion Scenarios for Engineering Applications: The Case of Thessaloniki, Greece. *Bulletin of the Seismological Society of America*, Vol. 98, pp. 1289-1303. doi: 10.1785/0120070114.
- Anastasiadis A, Raptakis D, Pitilakis K (2001). Thessaloniki's Detailed Microzoning: Subsurface Structure as Basis for Site Response Analysis. *Pure and Applied Geophysics*, Vol. 158, pp. 2597-2633. doi: 10.1007/pl00001188.
- Antonietti PF, Mazzieri I, Quarteroni A, Rapetti F (2012). Non-conforming High Order Approximations of the Elastodynamics Equation. *Computer Methods in Applied Mechanics and Engineering*, Vol. 209–212, pp. 212-238. doi: 10.1016/j.cma.2011.11.004.
- Apostolidis P, Raptakis D, Roumelioti Z, Pitilakis K (2004). Determination of S-wave Velocity Structure Using Microtremors and SPAC Method Applied in Thessaloniki (Greece). *Soil Dynamics and Earthquake Engineering*, Vol. 24, pp. 49-67. doi: 10.1016/j.soildyn.2003.09.001.
- Bielak J, Loukakis K, Hisada Y, Yoshimura C (2003). Domain Reduction Method for Three-Dimensional Earthquake Modeling in Localized Regions, Part I: Theory. *Bulletin of the Seismological Society of America*, Vol. 93, pp. 817-824. doi: 10.1785/0120010251.
- Borcherdt RD (1970) Effects of local geology on ground motion near San Francisco Bay. *B Seismol Soc Am* 60:29–6
- Castro, R. R., Pacor, F., Bindi, D., Franceschina, G. and Luzi, L. (2004). Site Response of Strong Motion Stations in the Umbria, Central Italy, Region. *Bulletin of the Seismological Society of America*, Vol. 94, pp. 576-590. doi: [10.1785/0120030114](https://doi.org/10.1785/0120030114)
- CEN (2004). Eurocode 8: Design Provisions for Earthquake Resistance of Structures, Part 1.1: General Rules, Seismic Actions and Rules for Buildings. European Committee for Standardization.
- Faccioli E, Vanini M, Paolucci R, Stupazzini M (2005). Reply to “Comment on ‘Domain Reduction Method for Three-Dimensional Earthquake Modeling in Localized Regions, Part I: Theory,’ by J. Bielak, K. Loukakis, Y. Hisada, and C. Yoshimura, and ‘Part II: Verification and Applications,’ by C. Yoshimura, J. Bielak, Y. Hisada, and A. Fernández”. *Bulletin of the Seismological Society of America*, Vol. 95, pp. 770-773. doi: 10.1785/0120040106.

- Haskell NA (1953). The Dispersion of Surface Waves on Multilayered Media. *Bulletin of the Seismological Society of America*, Vol. 43, pp. 17-34.
- Herrero A, Bernard P (1994). A kinematic Self-similar Rupture Process for Earthquakes. *Bulletin of the Seismological Society of America*, Vol. 84, pp. 1216-1228.
- Lachet C, Hatzfeld D, Bard PY, Theodulidis N, Papaioannou C, Savvaidis A (1996). Site Effects and Microzonation in the city of Thessaloniki (Greece) Comparison of Different Approaches. *Bulletin of the Seismological Society of America*, Vol. 86, pp. 1692-1703.
- Maufroy E, Chaljub E, Hollender F, Kristek J, Moczo P, Klin P, Priolo E, Iwaki A, Iwata T, Etienne V, De Martin F, Theodoulidis N, Manakou M, Guyonnet-Benaize C, Pitilakis K, Bard P-Y (2015) Earthquake ground motion in the Mygdonian basin, Greece: the E2VP verification and validation of 3D numerical simulation up to 4 Hz, *B Seismol Soc Am* 105(3): 1398–1418, doi: 10.1785/0120140228.
- Mazzieri I, Stupazzini M, Guidotti R, Smerzini C (2013). SPEED: SPECTral Elements in Elastodynamics with Discontinuous Galerkin: A Non-Conforming Approach for 3D Multi-Scale Problems. *International Journal for Numerical Methods in Engineering*, Vol. 95, pp. 991-1010. doi: 10.1002/nme.4532.
- Moczo P, Kristek J, Galis M (2014) The Finite-Difference modelling of earthquake motions: waves and ruptures. Cambridge University Press
- Olsen KB, Nigbor R, Konno T (2000). 3D viscoelastic wave propagation in the upper Borrego valley, California, constrained by borehole and surface data. *Bulletin of the Seismological Society of America*, Vol. 90, pp.134–150.
- Paolucci R (1999). Numerical Evaluation of the Effect of Cross-Coupling of Different Components of Ground Motion in Site Response Analyses. *Bulletin of the Seismological Society of America*, Vol. 89, pp. 877-887.
- Paolucci R, Mazzieri I, Smerzini C (2015) Anatomy of strong ground motion: near-source records and 3D physics-based numerical simulations of the Mw 6.0 May 29 2012 Po Plain earthquake, Italy. *Geophys J Int* 203:2001–2020. doi: 10.1093/gji/ggv405
- Pitilakis K, Riga E, Makra K, Gelagoti F, Ktenidou OJ, Anastasiadis A, Pitilakis D, Izquierdo Flores C (2014). Deliverable D11.5 Code Cross-Check, Computed Models and List of Available Results—AUTH Contribution. *Network of European Research Infrastructures for Earthquake Risk Assessment and Mitigation (NERA), 7th Framework Programme*. EC Project Number: 262330.
- Pitilakis K, Riga E, Anastasiadis A (2015). New Design Spectra in Eurocode 8 and Preliminary Application to the Seismic Risk of Thessaloniki, Greece. In: Ansal, A. and Sakr, M. (eds.) *Perspectives on Earthquake Geotechnical Engineering: In Honour of Prof. Kenji Ishihara*. Cham: Springer International Publishing. doi: 10.1007/978-3-319-10786-8_3.
- Roumelioti Z, Theodulidis N, Kiratzi A (2007). The 20 June 1978 Thessaloniki (Northern Greece) Earthquake Revisited: Slip Distribution and Forward Modelling of Geodetic and Seismological Observations. 4th International Conference on Earthquake Geotechnical Engineering, June 25–28 2007 Thessaloniki, Greece.
- Scandella L (2007). Numerical Evaluation of Transient Ground Strains for the Seismic Response Analysis of Underground Structures. *PhD Thesis*, Politecnico di Milano.
- Smerzini C., Paolucci R., Stupazzini M. (2011). Comparison of 3D, 2D and 1D numerical approaches to predict long period earthquake ground motion in the Gubbio plain, Central Italy. *Bulletin of Earthquake Engineering*, 9(6):2007–2029.
- Smerzini C, Pitilakis K, Hashemi K (2016). Evaluation of earthquake ground motion and site effects in the Thessaloniki urban area by 3D finite-fault numerical simulations. *Bulletin of Earthquake Engineering*, Vol. 15, Issue 3, pp. 787-812. doi: 10.1007/s10518-016-9977-5.
- Thomson WT (1950). Transmission of Elastic Waves through a Stratified Solid Medium. *Journal of Applied Physics*, Vol. 21, pp. 89-93. doi: 10.1063/1.1699629.